Available online at www.sciencedirect.com
ScienceDirect
Thermochimica Acta 470 (2008) 47–51
thermochimica acta
www.elsevier.com/locate/tca

Crystal structure and thermodynamic properties of cesium tantalum tungsten oxide

A.V. Knyazev *, N.G. Chernorukov, N.N. Smirnova, N.Yu. Kuznetsova, A.V. Markin

Nizhny Novgorod State University, Gagarin Prospekt 23/2, 603950 Nizhny Novgorod, Russia

Received 12 December 2007; received in revised form 18 January 2008; accepted 23 January 2008
Available online 5 February 2008

Abstract

In the present work temperature dependence of heat capacity of cesium tantalum tungsten oxide has been measured first in the range from 7 to 350 K and then between 330 and 630 K, respectively, by precision adiabatic vacuum and dynamic calorimetry. The experimental data were used to calculate standard thermodynamic functions, namely the heat capacity $C_p^\circ(T)$, enthalpy $H^\circ(T) - H^\circ(0)$, entropy $S^\circ(T) - S^\circ(0)$ and Gibbs function $G^\circ(T) - H^\circ(0)$, for the range from $T \to 0$ to 630 K. The structure of $CsTaWO_6$ is refined by the Rietveld method: space group $F\,d3m$, $Z = 8$, $a = 10.3793(2)$ Å, $V = 1118.14(4)$ Å^3. The high-temperature X-ray diffraction was used for the determination of temperature of phase transition and coefficient of thermal expansion.

Keywords: Cesium tantalum tungsten oxide; Adiabatic vacuum calorimetry; Heat capacity; Thermodynamic functions; X-ray diffraction

1. Introduction

Materials with the pyrochlore structure have been extensively studied for a range of applications including their use as adsorbents [1,2], radioactive waste form materials [3–5], as fast ion conductors [6], as Li-battery electrodes and, more recently, for photocatalytic splitting of water [7–10]. The pyrochlore structure type is also represented in a wide range of natural occurrences by the mineral group of pyrochlore, microlite, betafite and stibiconite [11].

The ideal defect pyrochlore structure has cubic symmetry (space group $F\,d3m$) and stoichiometry $A_2M_2X_6X'$ where A is a large, low valent cation (*e.g.* lanthanide or alkali metal or alkaline earth cation) and M is a smaller cation that can adopt octahedral coordination (*e.g.* Ti^{4+}, Zr^{4+}, W^{6+}, Sb^{6+}). Typically X is O^{2-} while X′ may be an anion such as O^{2-}, OH^- or F^-.

The goals of this work include calorimetric determination of the temperature dependence of the heat capacity $C_p^\circ = f(T)$ of cesium tantalum tungsten oxide from 7 to 630 K, detection of the possible phase transitions, and calculation of the standard thermodynamic functions $C_p^\circ(T)$, $H^\circ(T) - H^\circ(0)$, $S^\circ(T) - S^\circ(0)$ and $G^\circ(T) - H^\circ(0)$ in the range from $T \to 0$ to 630 K.

2. Experimental

2.1. Sample

Cesium tantalum tungsten oxide was prepared by the solid-state reaction between tungsten oxide, tantalum oxide and cesium nitrate [12]. The synthesis was performed in a porcelain crucible, into which the reaction mixture with the atomic ratio 1Cs:1W:1Ta was loaded. The mixture was calcined at 1073 K for 50 h, undergoing regrinding every 10 h.

For structural investigations, an X-ray diffraction pattern of a $CsTaWO_6$ sample was recorded on a Shimadzu X-ray diffractometer XRD-6000 (Cu Kα radiation, geometry θ–2θ) in the 2θ range from 10° to 120° with scan increment of 0.02°. Rietveld analysis and structure refinement [13] were carried out using RIETAN-94 software [14]. The X-ray data and estimated impurity content (0.5–1 wt%) in the substance led us to conclude that the cesium tantalum tungsten oxide sample studied was an individual crystalline compound. The high-temperature X-ray

* Corresponding author. Tel.: +7 831 465 62 06; fax: +7 831 434 50 56.
E-mail address: knav@uic.nnov.ru (A.V. Knyazev).

0040-6031/$ – see front matter © 2008 Published by Elsevier B.V.
doi:10.1016/j.tca.2008.01.017

diffraction was carried out on a Shimadzu X-ray diffractometer XRD-6000 using Sample Heating Attachment HA-1001.

2.2. Apparatus and measurement procedure

To measure the heat capacity C_p° of the tested substance in the range from 7 to 350 K a BKT-3.0 automatic precision adiabatic vacuum calorimeter with discrete heating was used. The calorimeter design and the operation procedure were described earlier [15,16]. The calorimeter was tested by measuring the heat capacity of high-purity copper and reference samples of synthetic corundum and K-2 benzoic acid. The analysis of the results showed that measurement error of the heat capacity of the substance at helium temperatures was within ±2%, then it decreased to ±0.5% as the temperature was rising to 40 K, and was equal to ±0.2% at $T > 40$ K. Temperatures of phase transitions can be determined with the error of ±0.02 K.

To measure the heat capacity of the sample between 330 and 630 K an automatic thermo-analytical complex (ADKTTM) – a dynamic calorimeter operating by the principle of triple thermal bridge – was employed [17,18]. The device design and the measurement procedure of the heat capacity, temperatures and enthalpies of phase transitions were demonstrated in detail in the above-mentioned papers. The reliability of the calorimeter operation was checked by measuring the heat capacity of the standard sample of synthetic corundum as well as the thermodynamic characteristics of fusion of indium, tin and lead. As a result, it was found that the calorimeter and the measurement technique allow one to obtain the heat capacity values of the substances in solid and liquid states with the maximum error of ±1.5% and the phase transition temperatures within *ca.* ±0.5 K. Since the heat capacity of the examined compound was also measured between 330 and 350 K in the adiabatic vacuum calorimeter with the error of ±0.2% and the conditions of measurements in the dynamic device were chosen so that in the above temperature interval the C_p° values measured with the use of both calorimeters coincided, it was assumed that at $T > 350$ K the heat capacity was determined with the error of 0.5–1.5%. The data on the heat capacity of the object under study were obtained in the range from 330 to 630 K at the average rate of heating of the calorimeter and the substance of 0.0333 K/s.

3. Results and discussion

3.1. Crystal structure

The structure of $CsTaWO_6$ was refined assuming space group *F d3m*. The initial model included the atomic coordinates in the structure of $CsNbWO_6$ [12]. The details of the X-ray diffraction experiment and structure refinement data are listed in Table 1.

Fig. 1 represents the measured, simulated, and difference X-ray diffraction patterns for $CsTaWO_6$, as well as a pattern of lines corresponding to reflection maxima. There is a good agreement between the measured and simulated patterns. Table 2 lists the coordinates of the atoms and their isotropic thermal parameters.

Table 1
Details of the X-ray diffraction experiment and the results of the structure refinement for $CsTaWO_6$

Space group	*F d3m*
Z	8
2θ range (°)	10–120
a (Å)	10.3793(2)
V (Å^3)	1118.14(4)
Number of reflections	73
Number of refined parameters:	
Structural parameters	4
Others	20
Final values (%):	
R_{wp}; R_p	3.22; 2.31

$$R_{wp} = \left\{ \frac{\sum w_i [y_{i\mathrm{obs}} - y_{i\mathrm{calc}}]^2}{\sum w_i [y_{i\mathrm{obs}}]^2} \right\}^{1/2}; \quad R_p = \frac{\sum |y_{i\mathrm{obs}} - y_{i\mathrm{calc}}|}{\sum y_{i\mathrm{obs}}}.$$

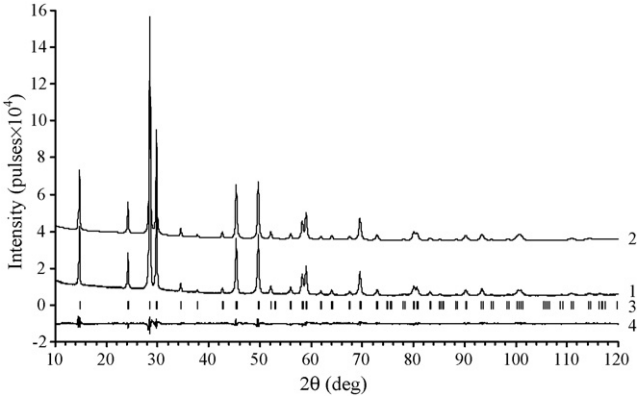

Fig. 1. Fragments of (1) observed, (2) simulated, and (4) difference X-ray diffraction patterns for $CsTaWO_6$ and (3) Bragg reflections. The simulated pattern is shifted relative to the observed pattern.

The refined model yielded positive isotropic thermal parameters B for all atoms. The Ta/W–O bond lengths are 1.966 ± 0.001 Å, and Cs–O bond lengths are 3.186 ± 0.004 Å.

Fig. 2 represents a fragment of the $CsTaWO_6$ structure. The $(Ta/W)O_6$ octahedra share corners to form a three-dimensional framework possessing tunnels running down the *c*-axis in which the Cs cations are located. The Ta/W cations are located in the 16c Wyckoff sites (0, 0, 0) and the oxygen atoms are in 48f sites (*x*, 1/8, 1/8). The location of the cesium cations is in the 8b sites (3/8, 3/8, 3/8).

Table 2
Coordinates and isotropic thermal parameters of atoms in the structure of $CsTaWO_6$

Atom	Site	*x*	*y*	*z*	Occ	*B* (Å^2)
Cs	8b	0.375	0.375	0.375		1.52(4)
Ta	16c	0	0	0	0.5	0.75(2)
W	16c	0	0	0	0.5	0.75(2)
O	48f	0.3180(4)	0.125	0.125		0.75(2)

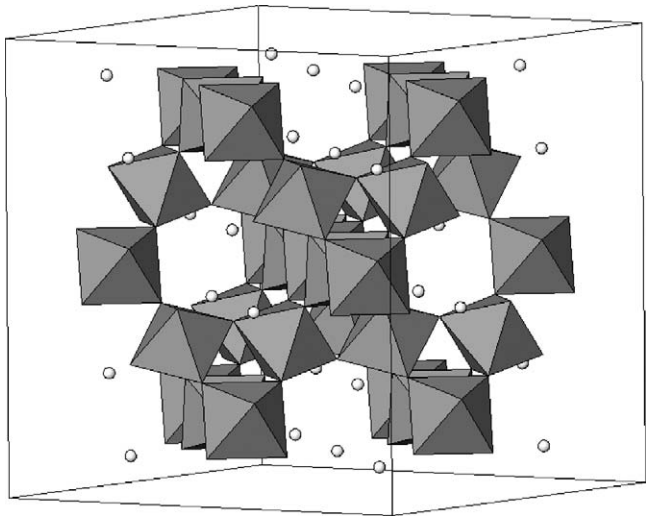

Fig. 2. Fragment of the structure of $CsTaWO_6$.

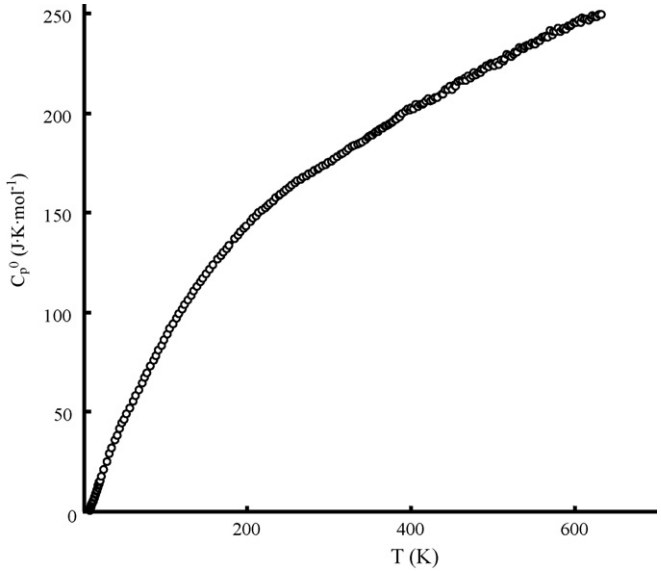

Fig. 3. Temperature dependence of heat capacity of $CsTaWO_6$.

3.2. Heat capacity

The C_p° measurements were carried out between 7 and 630 K. The masses of the sample loaded in the calorimetric ampoules of the BKT-3.0 and ADKTTM devices were 2.2184 and 2.1423 g, respectively. In the BKT-3.0 calorimeter, 121 experimental C_p° values were obtained in two series of experiments. The heat capacity of the sample varied from 30% to 70% of the total heat capacity of calorimetric ampoule + substance over the range between 7 and 630 K. The averaging of the experimental C_p° points in the region with no transformations was made in the form of degree and semilogarithmic polynomials, the corresponding coefficients were chosen by means of computer programs. So, for example, the following equations were used:

$$C_p^\circ = 9.6423 - 40.02\left(\frac{T}{30}\right) + 122.76\left(\frac{T}{30}\right)^2 - 97.599\left(\frac{T}{30}\right)^3 + 38.865\left(\frac{T}{30}\right)^4 - 7.6606\left(\frac{T}{30}\right)^5 + 0.59495\left(\frac{T}{30}\right)^6$$

in the range from $T = (25 \text{ to } 100)$ K;

$$C_p^\circ = -1.312792 \times 10^5 + 4.167009 \times 10^5 \ln\left(\frac{T}{30}\right) - 5.488911 \times 10^5 \ln^2\left(\frac{T}{30}\right) + 3.842331 \times 10^5 \ln^3\left(\frac{T}{30}\right) - 1.507253 \times 10^5 \ln^4\left(\frac{T}{30}\right) + 3.141533 \times 10^4 \ln^5\left(\frac{T}{30}\right) - 2.718069 \times 10^3 \ln^6\left(\frac{T}{30}\right)$$

in the range from $T = (150 \text{ to } 250)$ K.

In the above equations the C_p° is given in J K^{-1} mol^{-1} and T in Kelvin degree.

Their root mean square deviation from the averaging $C_p^\circ = f(T)$ curve was ±0.15% in the range $T = (6–40)$ K, ±0.075% from $T = (40 \text{ to } 80)$ K, ±0.050% between $T = (80 \text{ and } 350)$ K and ±0.5% over the range from $T = (350 \text{ to } 630)$ K.

The experimental values of the molar heat capacity of $CsTaWO_6$ over the range from 7 to 630 K and the averaging $C_p^\circ = f(T)$ plot are presented in Fig. 3. The heat capacity C_p° of this substance gradually increases with rising temperature and does not show any peculiarities until 630 K.

3.3. Standard thermodynamic functions

To calculate the standard thermodynamic functions (Table 3) of the cesium tantalum tungsten oxide, its C_p° values were extrapolated from the temperature of the measurement beginning at approximately 7–0 K by Debye's function of heat capacity:

$$C_p^\circ = nD\left(\frac{\theta_D}{T}\right), \quad (1)$$

where D is the symbol of Debye's function, $n = 5$ and $\theta_D = 100.6$ K are specially selected parameters. Eq. (1) with the above parameters describes the experimental C_p° values of the compound between 7 and 12 K with the error of ±1.0%. In calculating the functions it was assumed that Eq. (1) reproduces the C_p° values of $CsTaWO_6$ at $T < 7$ K with the same error. The calculations of $H^\circ(T) - H^\circ(0)$ and $S^\circ(T) - S^\circ(0)$ were made by the numerical integration of $C_p^\circ = f(T)$ and $C_p^\circ = f(\ln T)$ curves, respectively, and the Gibbs function $G^\circ(T) - H^\circ(0)$ was estimated from the enthalpies and entropies at the corresponding temperatures [19]. It was suggested that the error of the function values was ±1% at $T < 40$ K, ±0.5% between 40 and 80 K, ±0.2% in the range from 80 to 350 K and ±1.5% between 350 and 630 K.

The absolute entropies of cesium tantalum tungsten oxide (Table 3) and the corresponding simple substances W(cr), Ta (cr), Cs (cr) [20] and O_2 (g) [21] were used to

Table 3
Thermodynamic functions of crystalline $CsTaWO_6$; $M = 593.6997\ g\ mol^{-1}$, $p^\circ = 0.1\ MPa$

T (K)	$C_p^\circ(T)$ (J K^{-1} mol^{-1})	$H^\circ(T) - H^o(0)$ (kJ mol^{-1})	$S^\circ(T)$ (J K^{-1} mol^{-1})	$-[G^\circ(T) - H^\circ(0)]$ (kJ mol^{-1})
0	0	0	0	0
5	0.250	0.0000290	0.0566	0.000254
10	3.11	0.00707	0.901	0.00193
15	8.69	0.0358	3.16	0.0115
20	15.16	0.09544	6.543	0.03543
25	21.07	0.1863	10.57	0.07808
30	26.65	0.3056	14.91	0.1417
35	32.05	0.4525	19.43	0.2275
40	37.03	0.6255	24.04	0.3361
45	41.62	0.8219	28.66	0.4679
50	46.76	1.043	33.32	0.6228
55	50.56	1.287	37.96	0.8011
60	54.64	1.550	42.53	1.002
65	58.69	1.833	47.06	1.226
70	62.86	2.137	51.56	1.473
75	67.11	2.462	56.05	1.742
80	71.33	2.808	60.51	2.033
90	79.53	3.562	69.39	2.683
100	87.27	4.397	78.18	3.421
110	94.51	5.306	86.84	4.246
120	101.3	6.286	95.36	5.157
130	107.6	7.330	103.7	6.153
140	113.6	8.437	111.9	7.231
150	119.3	9.601	119.9	8.390
160	124.7	10.82	127.8	9.629
170	129.8	12.09	135.5	10.95
180	134.7	13.42	143.1	12.34
190	139.4	14.79	150.5	13.81
200	143.8	16.20	157.8	15.35
210	147.9	17.66	164.9	16.96
220	151.9	19.16	171.9	18.65
230	155.5	20.70	178.7	20.40
240	159.0	22.27	185.4	22.22
250	162.2	23.88	191.9	24.11
260	165.2	25.52	198.4	26.06
270	168.0	27.18	204.6	28.07
273.15	168.9	27.71	206.6	28.72
280	170.7	28.87	210.8	30.15
290	173.3	30.59	216.8	32.29
298.15	175.3	32.02	221.7	34.08
300	175.7	32.34	222.8	34.49
310	178.2	34.11	228.6	36.74
320	180.6	35.90	234.3	39.06
330	183.1	37.72	239.8	41.43
340	185.8	39.57	245.4	43.85
350	188.6	41.44	250.8	46.33
400	201.6	51.20	276.8	59.53
450	213.1	61.57	301.3	73.99
500	224.3	72.51	324.3	89.63
550	235.4	84.00	346.2	106.4
600	245.1	96.03	367.1	124.2
630	249.2	103.4	379.2	135.4

calculate the standard entropy of formation of the compound under study at 298.15 K, $\Delta_f S^\circ(298.15, CsTaWO_6, cr) = -553.2 \pm 2.1\ J\ K^{-1}\ mol^{-1}$.

3.4. High-temperature X-ray diffraction

The dependence of the unit cell parameter is plotted in Fig. 4 and Table 4, and it is described by the following square polynomial:

$$a = 1.68 \cdot 10^{-8} \cdot T^2 + 3.89 \cdot 10^{-5} \cdot T + 10.3681 (298 \leq T \leq 1073\ K). \quad (2)$$

The average thermal expansion coefficient $\alpha_{av} = 5.92 \times 10^{-6}\ K^{-1}$ obtained for the cesium tantalum

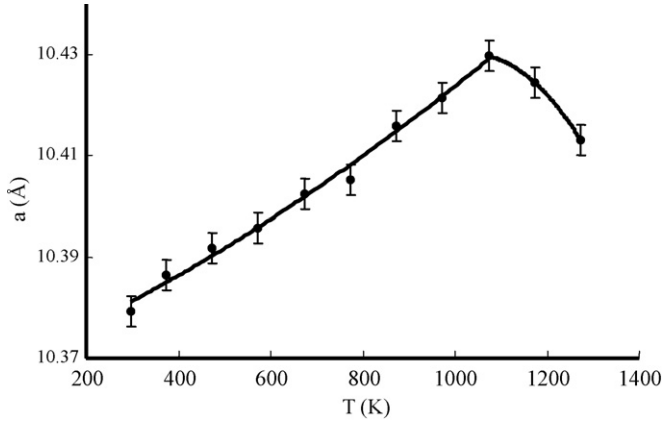

Fig. 4. Plot of unit cell parameter vs. temperature for $CsTaWO_6$.

Table 4
Parameters of unit cells and thermal expansion coefficients vs. temperature for $CsTaWO_6$

T (K)	a (Å)	V (Å^3)	ρ (g cm^{-3})	α ($\times 10^6$ K^{-1})
298	10.3793(2)	1118.14(4)	7.051	4.71
373	10.3865(9)	1120.5(3)	7.036	4.95
473	10.3917(8)	1122.2(3)	7.026	5.27
573	10.3958(8)	1123.5(3)	7.018	5.59
673	10.4025(9)	1125.7(3)	7.004	5.91
773	10.4053(9)	1126.6(3)	6.998	6.23
873	10.4159(8)	1130.0(3)	6.977	6.55
973	10.4214(9)	1131.8(3)	6.966	6.87
1073	10.4297(9)	1134.5(3)	6.950	7.19
1173	10.4245(8)	1132.8(3)	6.960	–
1273	10.4131(9)	1129.1(3)	6.983	–

tungsten oxide under investigation allows us to assign this pyrochlore to the class of medium-expansion compounds. In the range 1073–1123 K, a "break" is observed in the $a = f(T)$ curve for $CsTaWO_6$ due to crystal I (cubic) → crystal II (cubic) reversible transition. Physically, the anomaly can be related to the changing of cesium crystallographic position from 8b (3/8, 3/8, 3/8) to 32e (x, x, x) [22].

Acknowledgement

The work was performed with the financial support of NNSU's innovation educational program within the National project "Education".

Appendix A. Supplementary data

Supplementary data associated with this article can be found, in the online version, at doi:10.1016/j.tca.2008.01.017.

References

[1] L.G. Nagy, G. Torok, G. Foti, Proc. Int. Conf. Colloid Surf. Sci. (1975) 33.
[2] M. Abe, T. Kotani, S. Awano, in: P.A. Williams, A. Dyer (Eds.), Advances in Ion Exchange for Industry and Research, vol. 239, Special Publication, Royal Society of Chemistry, Cambridge, 1999, p. 199.
[3] R.C. Ewing, W.J. Weber, J. Lian, J. Appl. Phys. 95 (2004) 5949.
[4] R.C. Ewing, W.J. Weber, W. Lutze, NATO ASI Series 1: Disarmament Technologies, 4, 1996, 65.
[5] R.C. Ewing, Can. Mineral. 39 (2001) 697.
[6] W.A. England, M.G. Cross, A. Hamnett, P.J. Wiseman, J.B. Goodenough, Solid State Ionics 1 (1980) 231.
[7] J. Wang, Z. Zou, J. Ye, Mater. Sci. Forum (2003) 423.
[8] Z.G. Zou, H. Arakawa, J. Photochem. Photobiol. A 158 (2003) 145.
[9] Z. Zou, J. Ye, H. Arakawa, J. Mol. Catal. A: Chem. 168 (2001) 289.
[10] Z. Zou, J. Ye, H. Arakawa, Int. J. Hydrogen Energy 28 (2003) 663.
[11] M. Fleischer, Glossary of Mineral Species 1983, Mineralogical Record, Tucson, 1983.
[12] D. Babel, D. Pausewang, W. Viebahn, Zeitschrift fuer Naturforschung Teil B 22 (1967) 1219.
[13] H.M. Rietveld, Acta Crystallogr. 22 (Part 1) (1967) 151.
[14] F. Izumi, R.A.Young, The Rietveld Method, Oxford University Press, Oxford, chap. 13, 1993.
[15] R.M. Varushchenko, A.I. Druzhinina, E.L. Sorkin, J. Chem. Thermodyn. 29 (1997) 623.
[16] V.M. Malyshev, G.A. Milner, E.L. Sorkin, V.F. Shibakin, Pribory i Tekhnika Eksperi-menta 6 (1985) 195.
[17] M.Sh. Yagfarov, Zh. Fiz, Khimii 43 (1969) 1620.
[18] A.G. Kabo, V.V. Diky, Thermochim. Acta 347 (2000) 79.
[19] B.V. Lebedev, Thermochim. Acta 297 (1997) 143.
[20] M.W. ChaseJr., J. Phys. Chem. Ref. Data, Monograph, 9, 1998, 1951.
[21] J.D. Cox, D.D. Wagman, V.A. Medvedev, Codata Key Values for Thermodynamics, Hemisphere Publishing Corrp., New York, 1984, p. 1.
[22] V. Luca, C.S. Griffith, M.C. Blackford, J.V. Hanna, J. Mater. Chem. 15 (2005) 564.